Gap-state density of lightly P- and B-doped *a*-Si:H deduced from space-charge-limited photocurrents

H. Kakinuma, M. Mohri, M. Sakamoto, and H. Sawai
Research Laboratory, Oki Electric Industry Co., Ltd., Higashiasakawa 550-5, Hachioji, Tokyo 193, Japan
(Received 24 September 1990)

The gap-state density of lightly P- and B-doped *a*-Si:H has been deduced from space-charge-limited-photocurrent (SCLPC) measurements under blue-light ($\lambda=450$ nm) illumination. The sample structures used (Schottky or back-to-back heterodiodes) completely eliminate the problem of active impurity (P or B) contamination, which could not be excluded in the conventional space-charge-limited-current measurements. First, we discuss the principle of this technique and postulate the conditions for deducing a meaningful expression for the density of states $g(E)$. The validity of the deduced $g(E)$ is experimentally verified. The energy profiles of $g(E)$ for lightly P- [1–10 vppm in the gas phase (vppm = volume parts per million)] and B-doped (3–6 vppm) *a*-Si:H deduced from SCLPC prove to be qualitatively similar to those deduced from deep-level transient spectroscopy, the constant-photocurrent method, and photothermal deflection spectroscopy; $g(E)$ below (above) the intrinsic Fermi level E_{f0} is much larger than that above (below) it for P- (B-) doped films. However, the energy profile around E_{f0} for 0.5 vppm B_2H_6-doped films shows a low and almost flat [$(3-5)\times10^{15}$ cm^{-3}eV^{-1}] density of states. This doping-induced modification in $g(E)$ is discussed based on the existing data and models.

I. INTRODUCTION

The density of states (DOS) in the band gap of amorphous silicon (*a*-Si:H) is a basic quantity for the understanding and application of the material. The space-charge-limited (dark) current (SCLC) has been applied to the determination of the energy profiles of the DOS, particularly in the midgap region.[1–4] In this method, superlinear current-voltage (I-V) characteristics due to injected charges from Ohmic contacts are measured. However, a high-level doping of phosphorus or boron to make the contacts can contaminate the undoped layer subsequently deposited.[3] To dispense with the n^+-type or p^+-type layers, we recently proposed a kind of SCLC technique, space-charge-limited photocurrent (SCLPC),[5] which uses blocking (Schottky or hetero) contacts, and photogenerated carriers as a source of space charge. Although SCLPC itself has been studied from the 1960s for other photoconductors[6,7] and recently for *a*-Si:H,[8,9] there has been no attempt to deduce the DOS from it. In this technique, dopant contamination essentially does not occur. The DOS derived from the technique proved to be similar to that from the conventional SCLC technique.

The previous work, however, was limited to undoped *a*-Si:H. In this paper, we describe on the results lightly phosphorus and boron doped *a*-Si:H films, including a detailed and comprehensive description of this technique. It has been shown that the light doping (in particular, B doping) into *a*-Si:H is very important in optoelectronic devices such as solar cells and image sensors.[10,11] First we describe the technique in detail in Sec. II, including conditions for meaningful measurement, factors that might affect the deduced DOS, and also the sample structures specific to the dopant types. In Sec. III, the obtained energy profiles of the DOS for the undoped and lightly P- and B-doped *a*-Si:H will be shown. Finally we will discuss in Sec. IV the doping-induced change in the energy profiles of the DOS found by the SCLPC technique, comparing with existing data and models.

II. THE SCLPC TECHNIQUE

A. Conditions for the SCLPC technique

In the SCLPC technique, the source of the space charge is not injected charges from an upstream contact but photogenerated charges, as is schematically illustrated in Fig. 1. The excitation light is illuminated through the top indium tin oxide (ITO) contact. The DOS is calculated from the photocurrent-voltage (I_{ph}-V) characteristics. Here, V is the bias voltage defined as $V_A-\Delta V$, where V_A is the applied voltage and ΔV is the voltage offset at $I_{ph}=0$. To ensure the formation of a unipolar space charge in the bulk region, both contacts must be of the blocking type so that injection from the contacts may be neglected. Experimentally, the dark current I_d must be sufficiently lower than I_{ph}, i.e., $I_d \ll I_{ph}$ (condition 1).

Furthermore, the perturbation in the boundary regions should be minimized for the precise determination of $g(E)$. Therefore, strongly absorbing light is used in the SCLPC technique, i.e., $\alpha L \gg 1$ (condition 2), where α is the absorption of *a*-Si:H and L is the film thickness.

Another important factor in the forming of a uniform space charge is the magnitude of the range ($\mu\tau F$) of the photocarriers. Here μ is the mobility, τ is the deep-trapping time, and F is the electric field. If the $\mu\tau F$ is so large as to become some portion of L, the space charge is substantially not formed there. In this region, the elec-

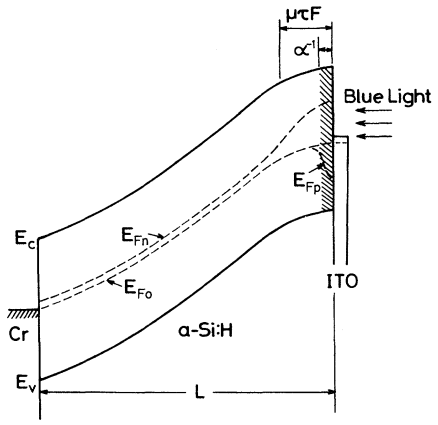

FIG. 1. Schematic band diagram of a Cr/*a*-Si:H/ITO Schottky photodiode under a bias voltage in the case of electron space charge. The hatched region indicates a light-absorbing region.

tron density n in the conduction band and tail states is much larger than deeply trapped electrons N_t, and therefore, they are far from equilibrium. A large value of $\mu\tau F$ also causes a large electric field nonuniformity, as is clear from the current continuity equation. Thus the $\mu\tau F$ must be much smaller than L, i.e., $\mu\tau F \ll L$, to ensure the space-charge uniformity (condition 3). In device-quality *a*-Si:H films, condition 3 is not always satisfied because of large values of $\mu\tau$. In this case, another thin layer, in which $\mu\tau$ is so small as to satisfy condition 3, should be interposed between the intrinsic layer and the transparent contact to minimize the nonequilibrium region. The structure of samples will be described in detail later.

In the transition region, the nonequilibrium (light-absorbing) region gradually changes to the space-charge (bulk) region in reality. However, for simplicity, we assume that the two regions are electrically uniform and its boundary is broken. The photocurrent density J ($=I_{\rm ph}/A$, where A is the diode area) in the two regions is connected by the current continuity equation,

$$\begin{aligned} J &= e(n_1\mu_n + p_1\mu_p)F_1 \\ &= e(\mu_n\tau_n + \mu_p\tau_p)GF_1 \\ &= en_2\mu_n F_2 \ , \end{aligned} \tag{1}$$

$$n_2 = N_c \exp[-(E - E_{fn})/kT] \ , \tag{2}$$

where e is the electron charge, n and p are the free-electron and hole densities, μ is the mobility, τ is the recombination life time, G is the photocarrier generation rate, N_c is the effective density of states in the conduction band, E_{fn} is the quasi-Fermi-level for electrons, k is Boltzmann's constant, and T is the absolute temperature. The subscripts n and p stand for electrons and holes, respectively, and 1 and 2 denote the light-absorbing and bulk regions, respectively. Since we can assume $n_2\mu_n \ll (n_1\mu_n + p_1\mu_p)$, F_1 is much smaller than F_2 ($\simeq V/L$). Consequently, one can regard the photogeneration region as a charge reservoir with negligible thickness. The reservoir provides as much charge as the space-charge layer requires so that the boundary condition, $F_1 = 0$ at the upstream contact usually assumed in SCLC, may virtually apply. However, if the charge required by the space-charge region exceeds the generated charge by an increased V, current saturation will occur.

In the space-charge region, the energy distribution of electrons is assumed to be under quasiequilibrium according to the Fermi statistics. The density of electrons at an energy E, $n(E)$, is given by

$$n(E) = g(E)f(E) \ , \tag{3}$$

where $f(E)$ is the Fermi distribution function,

$$f(E) = \{\exp[(E - E_{fn})/kT] + 1\}^{-1} \ . \tag{4}$$

Using these equations, N_t is expressed as

$$N_t \simeq \int_{E_{f0}}^{E_{fn}} g(E)f(E)dE \ , \tag{5}$$

where E_{f0} is the intrinsic Fermi level without illumination. The E_{fn} (i.e., N_t) increases with increasing light illumination. Under a constant intensity illumination (i.e., a constant N_t), the shift in E_{fn} reduces as $g(E)$ increases. An increase in V also increases E_{fn} as in the usual SCLC. Similar expressions apply in the case of holes ($E < E_{f0}$).

B. Photocurrent-voltage characteristics

We first examined the effect of incident-light wavelength λ on $I_{\rm ph}$. The $I_{\rm ph}$-V characteristics were measured with a picoammeter (YHP-4140B). The top ITO contact was biased negative (positive) for electron (hole) current measurements under illumination. A monochrometer was used to obtain monochrome lights with an intensity range of 2–100 μW/cm^2. The $I_{\rm ph}$-V characteristics for four wavelengths are shown in Fig. 2. It can be seen that the I_d is sufficiently low even at high bias voltages, indicating that current injection from the contacts is well blocked. For a long wavelength of 660 nm, no space-charge-limited photocurrent is observed. When the wavelength becomes short, the photocurrent becomes space-charge limited, and below 500 nm the shapes of the curves are substantially the same. From this result, we adopted 450 nm as a wavelength of incident light. With decreasing wavelength, the penetration depth α^{-1} becomes small, and the space charge region spreads throughout the whole film. The α^{-1} value of our *a*-Si:H films for 450 nm is approximately 50 nm, which satisfies condition 2.

Figure 3 shows $I_{\rm ph}$-V characteristics under varied light intensities (2~103 μW/cm^2). The curve monotonically shifts upwards with increased light intensity. Also, there are indications of current saturation for all light intensities at V larger than approximately 10 V. However, the light intensity dependence of $I_{\rm ph}$ is not linear for $V < 10$ V, i.e.,

$$I_{\rm ph} \propto G^{\gamma} \ (0.5 < \gamma < 1) \tag{6}$$

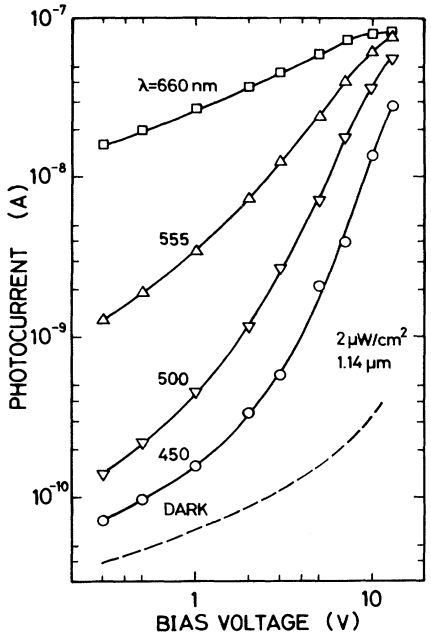

FIG. 2. Bias-voltage dependence of hole photocurrents for various incident-light wavelengths, including that of dark current.

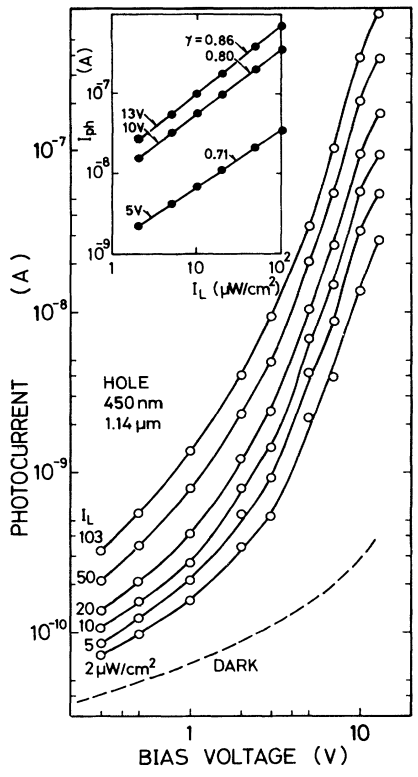

FIG. 3. Bias-voltage dependence of photocurrents for various incident-light intensities. The inset is the illumination-intensity dependence of photocurrents at three bias voltages with γ values ($I_{ph} \propto I_L^{\gamma}$).

as can be seen in the inset of Fig. 3 despite the primary photocurrent. Furthermore, γ decreases as V decreases. This may be due to the fact, $F_1 \ll F_2$ as is clear from Eq. (1). It has been suggested that the light-intensity dependence of photocurrent is not linear even for primary photocurrents when electric field strength is weak.[12]

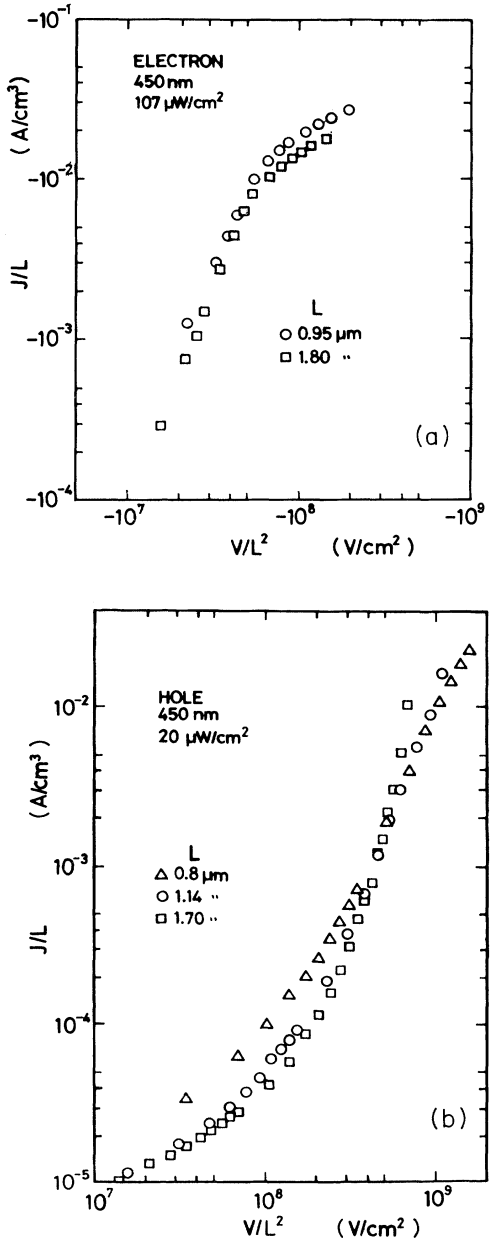

FIG. 4. $J/L - V/L^2$ (scaling law) plots of photocurrents for samples with different thicknesses. (a) Electron current (b) hole current (reproduced from Ref. 5).

C. Scaling law

The most efficient test for the uniform formation of space-charge or bulk-controlled photocurrent is applicability of an universal scaling law,[13]

$$J/L = f(V/L^2), \tag{7}$$

where f is an adequate function. Figures 4(a) and 4(b) show the J/L versus V/L^2 plots for samples prepared under the same condition but with different thicknesses. In the conventional SCLC measurements, it is known that unintentional deviation of plasma conditions or residual impurities induces a disagreement with the scaling law.[2,3] However, it can be seen that plots lie fairly well on a common curve, indicating that the currents are bulk controlled.

D. Sample structures

The sample structure used for the SCLPC measurements is basically a-Si:H films sandwiched by Cr and ITO electrodes as previously shown. Both electrodes form Schottky contacts against a-Si:H. The a-Si:H films were deposited on Cr-coated Corning 7059 substrates by rf decomposition of SiH_4 under an optimized condition similar to our previous work.[14] ITO transparent dots were made on the film surface. The total thickness of the a-Si:H was from 0.8 to 1.25 μm.

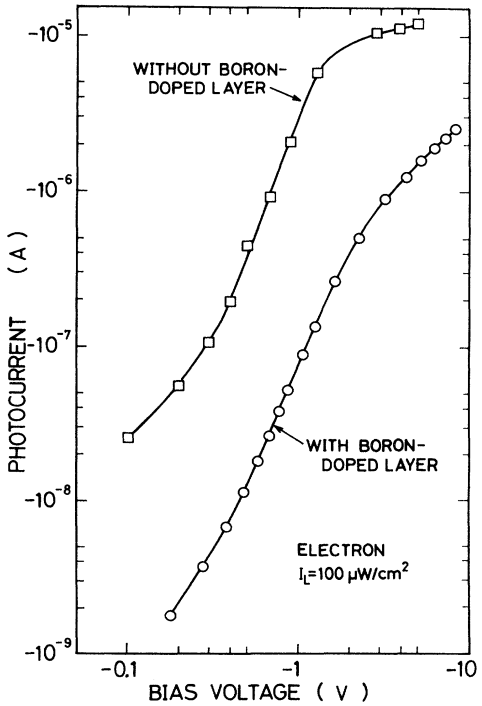

FIG. 5. Bias-voltage dependence of photocurrents for two kinds of samples: one with a thin lightly B-doped layer (100 nm; $[B_2H_6]/[SiH_4]=6$ vppm) interposed between the ITO and a-Si:H layers, and one without the B-doped layer.

TABLE I. Sample structures.

Space charge Dopant	Holes	Electrons
P	Cr/SiO_2/ν/ITO	Cr/ν/p^-[a]/ITO
Undoped	Cr/i/ITO	Cr/i/p^-/ITO
B	Cr/π/ITO	Cr/π/p^-/ITO

[a] p^- denotes a thin B-doped layer (100 nm; $[B_2H_6]/[SiH_4]=6$ vppm).

As was explained above, a carrier trapping layer is required to reduce the range of photocarriers if it is not negligible compared to L. In a previous paper, we found that the electron $\mu\tau$ value (2×10^{-8} cm^2 eV^{-1}) of the undoped sample is one order-of-magnitude larger than that for holes (2×10^{-9} cm^2 eV^{-1}), and that 6 vppm (vppm is volume parts per million) B_2H_6 doping reduces the electron $\mu\tau$ value to 2×10^{-9} cm^2 eV^{-1}.[14] The $\mu\tau F$ for the B-doped a-Si:H becomes about 0.1 μm or less for an applied voltage of 1 V. Hence, we used 6-vppm B_2H_6-doped a-Si:H layers of 0.1-μm thickness as electron trapping layers for the measurements of electron photocurrent.

The effect of interposing the electron trapping layer is shown in Fig. 5. The I_{ph} with the trapping layer is more than one order-of-magnitude smaller than that of the diode without the layer. This indicates that a large part of the photocarriers (electrons) are trapped in the lightly B-doped layer. Once trapped, the free carriers and trapped carriers are considered to be under quasiequilibrium according to Eq. (4). The nominally deduced $g(E)$ value from the I_{ph}-V curve for the sample without the trapping layer is in the 10^{14} cm^{-3} eV^{-1} range, which is unrealistically small.

When the ITO electrode is positively biased with respect to the Cr electrode for the lightly P-doped sample, injection of electrons increased significantly. Then a thin SiO_2 layer of about 10 nm thick, made by rf decomposition of SiH_4 and N_2O, was interposed between the Cr and a-Si:H layers. The sample structures used for the present measurements are summarized in Table I.

E. Calculation of $g(E)$

The calculation methods for deriving $g(E)$ from the I-V curves in the SCLC techniques, such as the the step-by-step method and the differential method, have been developed by den Boer, and Nešpurek and Sworakowski, respectively.[1,15] Since there is no difference in the carrier transport between the SCLC and SCLPC techniques except for the source of space charges, both methods can apply to the calculation. We calculated $g(E)$ using the differential method here. According to the method, $g(E)$ and E are given by

$$g(E)=\frac{\chi_1\epsilon_0\epsilon}{eL^2kT}\frac{V}{m(V)-1},\quad m(V)=\frac{d(\log_{10}J)}{d(\log_{10}V)}, \tag{8}$$

$$E_c-E=kT\ln(eN_c\mu_c\chi_2/L)+kT(V/J),\quad E_{f0}<E \tag{9a}$$

$$E-E_v=kT\ln(eN_v\mu_v\chi_2/L)+kT(V/J),\quad E<E_{f0} \tag{9b}$$

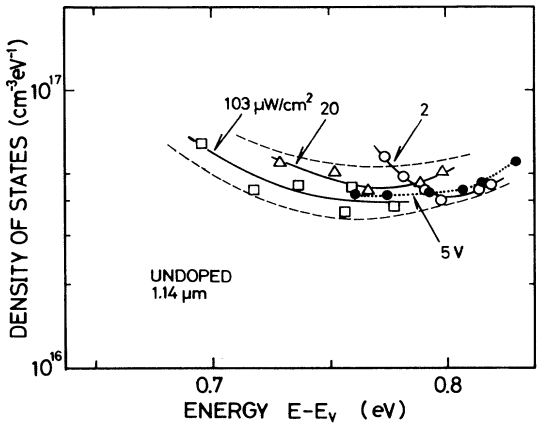

FIG. 6. Energy profiles of the density-of-states of undoped a-Si:H deduced from different I_{ph}-V curves under three different (2, 20, 103 μW/cm^2) light intensities (Fig. 3) and from varied light intensity at $V=5$ V.

where ϵ is the dielectric constant, ϵ_0 is the permittivity of free space, χ_1 and χ_2 are correction factors for the nonuniformity of the internal field and the carrier density, and are set 0.75 and 1 here, respectively.[2] In order to determine the energy scale relative to E_c or E_v, knowledge of the values of the effective density of states N_c and N_v, microscopic mobilities μ_c and μ_v are necessary. The subscripts c and v denote the conduction and valence bands, respectively. Here, we employed the values of $g(E_c)$ and $g(E_v)$ as 4×10^{21} cm^{-3}eV^{-1}, and then N_c and N_v as 1×10^{20} cm^{-3} from the relation, $N_{c,v}=kTg(E_{c,v})$.[16] These values are those measured by optical methods and appear to be most reliable at the present stage. μ_c and μ_v were set to 10 cm^{2}V^{-1}s^{-1}.[17]

We calculated $g(E)$'s from three different I_{ph} curves of Fig. 3 (2, 20, 103 μW/cm^2) using Eqs. (8) and (9), and the result is shown by open symbols in Fig. 6. As the illumination intensity (i.e., I_{ph}) increases, the energy range shifts towards the valence band, as is clear from Eq. (9). It should be noted that, although the energy range probed shifts, the $g(E)$ values for each illumination continuously overlap. The scattering in $g(E)$ due to the difference in illumination intensity is estimated to be within a factor of about 2. In the SCLPC measurement, there is another measurement method in which the illumination intensity is varied under a constant bias voltage. The solid circles in Fig. 6 are the plots derived by the latter method under a constant bias voltage of 5 V. To cover a wider range of the energy scale, particularly for the smaller $E-E_v$, E_c-E range, use of more intense light such as a He-Cd laser is required.

III. DEDUCED DENSITY OF STATES

A. Thickness dependence

It has been shown that the DOS deduced from SCLC measurements is film-thickness dependent, i.e., a larger DOS for thinner films.[3,4] Figure 7 shows the thickness dependence of the DOS at $E-E_v=0.74$ eV deduced by the SCLPC for undoped films. It can be seen that $g(E)$ increases with decreasing thickness, particularly below approximately 1 μm. This tendency is qualitatively in agreement with other results mentioned above. However, the rate of the change in $g(E)$ with thickness is larger for our data than those of others by a factor of about 2. It should be pointed out that there are differences in the measurement condition between our experiment and others; firstly, $g(E)$ of our data is that of the valence-band side of the E_{f0}, and secondly, it is at a constant energy ($E-E_v=0.74$ eV).

As will be shown in Sec. III B, the $g(E)$ below the E_{f0} is larger than that above it for the undoped sample. If the main defect of undoped a-Si:H is the dangling-bond states located below E_{f0}, as is widely accepted, probing the energy region below E_{f0} would be more sensitive to the change in the defect density associated with the film thickness, which may explain the larger thickness dependence shown in Fig. 7. Other data probing the DOS such as subband absorption or electron spin resonance have indicated that the DOS for thin films is large as compared to thicker films,[18,19] probably due to the more disordered structure in the vicinity of substrates and evolutional relaxation of the structure during the film growth.

Secondly, the previous data on the thickness dependence of $g(E)$ (Refs. 3 and 4) is generally at new Fermi levels E_{fn} (E_{fp}) shifted by the formation of the space charge so that it is not at a constant level. As $g(E)$ becomes larger, E_{fn} (E_{fp}) will shift towards E_{f0} where $g(E)$ is generally smaller than E_{fn} (E_{fp}), resulting in a weakening in the change of $g(E)$.

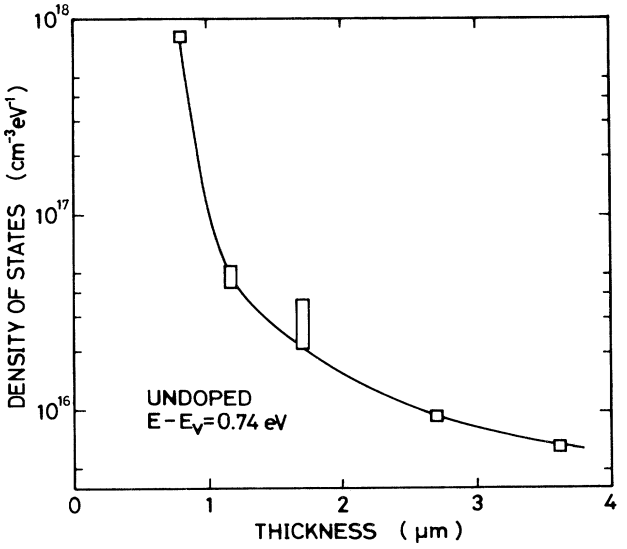

FIG. 7. Thickness dependence of the density-of-states $g(E)$ of undoped a-Si:H at a constant energy ($E-E_v=0.74$ eV).

B. $g(E)$ profiles of lightly P- and B-doped a-Si:H

The DOS of lightly P- and B-doped a-Si:H has also been obtained by conventional SCLC techniques using n^+-i-n^+ or p^+-i-p^+ samples.[4] However, these structures will not completely exclude the effects of dopant contamination because only slight doping (<1 ppm) could change the shape of $g(E)$, particularly for B doping, as will be shown in the following.

Figure 8 shows the energy profiles of lightly P- and B-doped samples together with that of an undoped one. The numbers N in the figure (PN, BN) denote the gas-phase-dopant mixing ratios, $[PH_3]/[SiH_4]$ and $[B_2H_6]/[SiH_4]$, respectively. As can be seen in the figure, the $g(E)$ in the region below E_{f0}, $g(E<E_{f0})$, is one order of magnitude larger than that in the region above E_{f0}, $g(E>E_{f0})$ for the undoped sample. A 1-vppm PH_3 doping further increases $g(E<E_{f0})$, while it reduces $g(E>E_{f0})$. As for B-doping, there has been no data on the energy profile of $g(E)$, as far as we know, particularly for the doping levels smaller than a few ppm. In contrast with P doping, light B doping reduces $g(E<E_{f0})$, while it increases $g(E>E_{f0})$. The reduction in $g(E<E_{f0})$ by the B doping appears to saturate above the doping level of 3 vppm, while the increase in $g(E>E_{f0})$ continues with further doping. A low and almost flat distribution of $g(E)$ $[(3\sim5)\times10^{15}\ \mathrm{cm^{-3}eV^{-1}}]$ around midgap, i.e., an electrically intrinsic condition, is achieved at the doping level of about 0.5 vppm. This is in good agreement with the result that the transport properties of electron and holes are optimized by the B doping at this doping level.[14]

IV. DISCUSSION

The overall trend of the energy profiles of $g(E)$ for our undoped and lightly P- and B-doped a-Si:H is remarkably similar to those for more heavily doped films obtained from other measurements such as deep-level transient spectroscopy[20] (DLTS) or recent data of the constant-photocurrent method (CPM) and photothermal deflection spectroscopy (PDS).[21–23] The DLTS data for undoped and P-doped samples showed that $g(E<E_{f0})$ is much larger than $g(E>E_{f0})$, and that $g(E<E_{f0})$ increased with increasing doping level. The values of $g(E<E_{f0})$ for undoped samples are similar to ours ($\simeq4\times10^{16}$ $\mathrm{cm^{-3}eV^{-1}}$). Differences are the magnitude of $g(E)$ and energy level at which the $g(E>E_{f0})$ takes minimum values, i.e., $g(E)\simeq2\times10^{15}\ \mathrm{cm^{-3}eV^{-1}}$ at $E_c-E\simeq0.7$ eV for our measurement and $g(E)<10^{15}\ \mathrm{cm^{-3}eV^{-1}}$ at $E_c-E\simeq0.5$ eV for the DLTS measurement.[20] CPM and PDS measurements also showed that $g(E<E_{f0})$ increased with increasing PH_3 doping level (30$\sim$3000 vppm), while $g(E>E_{f0})$ decreased with increasing doping level.[21–23]

The CPM and PDS techniques require deconvolution of the optical-absorption spectra and so accompanies some uncertainty due to assumed parameters.[24] In contrast, the SCLPC technique is a more direct method with few mathematical manipulations. Therefore, we may say that the changes in $g(E)$ by P- and B-doping derived by these methods are confirmed by the present data and proved to be universal.

A model explaining the doping-induced change in $g(E)$ has been presented by Kočka.[25] The model is based on the assumption that doping creates dopant-defect complexes, P_4^+-D^- and B_4^--D^+, and Coulomb interaction between the charged atoms lowers the energy of the charged-D states relative to the conduction and valence bands, respectively. Recently, Winer has developed a thermodynamical model where defects are created in order to minimize the system-free energy, and the defect chemical potential depends on the Fermi energy.[26] This model does not necessarily require the defect complexes and accounts for the temperature dependence of the defect concentration. In any case, both models predict that the D^- states for the P-doped sample are located below E_{f0}, while the D^+ states for the B-doped samples are located above E_{f0}. These models generally account for the tendency of our data, although the energy positions of the maximum of the DOS in the present data is not identified because of the limited energy range that the present SCLPC covered. According to these models, the bump below E_{f0} found for the undoped sample (Fig. 8) corresponds to the D^0 state while that for the PH_3-doped samples corresponds to the D^- state. Both states form a positive charge in the bulk as D^+ and P_4^+, respectively, by hole trapping. According to the Winer's model where the energy level of the D states is dependent on the Fermi level, the energy level of the D states will continuously decrease with an increasing P-doping level. However, if the large bump in $g(E<E_{f0})$ for the P-doped sample is assigned to the D^- states, it may be concluded that the decrease in the energy of the D^- states occurs rather abruptly at a smaller doping level than 1 vppm. The slight shift in the high-energy shoulder of $g(E<E_{f0})$ with an increasing P-doping level (Fig. 8) may correspond

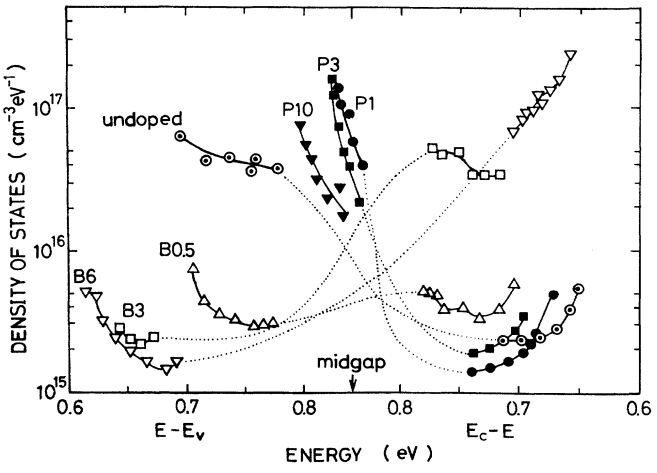

FIG. 8. Energy profiles of the density-of-states $g(E)$ for undoped and P- and B-doped a-Si:H. The numbers N in PN or BN denote the gas-phase doping level ($[PH_3]/[SiH_4]$, $[B_2H_6]/[SiH_4]$) in vppm.

to the predicted shift.

The increase in $g(E)$ above E_{f0} with the B_2H_6 doping larger than 3 vppm can be understood by the Kočka's or Winer's model. However, more detailed consideration should be given to the "decrease" in $g(E<E_{f0})$ by the 0.5-vppm doping. If the B doping simply creates the D^+-B_4^- pairs as the Kočka's model suggests, the density of intrinsic D states below E_{f0} will not change because the pair D^+ state is assumed to be located above E_{f0}, which disagrees with the results shown in Fig. 8. On the other hand, according to the Winer's model, the decrease in $g(E<E_{f0})$ may be attributed to the shift of the energy level of the D^0 states towards the conduction band, if we assume that additional D states are not formed by B doping. However, no large bump comparable to that for the undoped sample is identified in the energy profile of the 0.5-vppm B_2H_6-doped sample. If additional D^+ states are created by the B doping below E_{f0}, one cannot "see" the D^+ states located below E_{f0} by the SCLPC technique because they no longer trap holes. Also in this case, however, the density of the D^0 states will not change. In contrast, if the D^+ states are created above E_{f0}, one would see them because they can trap electrons, but this disagrees with the result. Thus it is difficult to account for the decrease in $g(E<E_{f0})$ for the 0.5-vppm-doped sample by the existing models shown in Fig. 8.

One explanation for the decrease in $g(E<E_{f0})$ is defect compensation by the dopant (B) atoms. However, 0.5-vppm B_2H_6 doping corresponds to only a 3×10^{16} cm^{-3} B concentration in the *a*-Si:H film.[27] It is very unlikely that most of the B atoms happen to be incorporated to the dangling-bond sites. Another possible explanation is the one we previously proposed.[14] We assumed that B atoms are incorporated simply as B_4 states without forming additional D states as long as its concentration is lower than that of the intrinsic D^0 states. The holes emitted from the B_4 states will convert the D^0 states to D^+ states by trapping. Consequently, the intrinsic D^0 states are more and more converted to D^+ states with increasing B-doping level and consequently, become unobservable as explained above. This naturally accounts for the decrease in $g(E<E_{f0})$ by B doping. The subband absorption experiments such as CPM or PDS will also not see the D^+ states located below E_{f0}, since they observe electron transition from occupied states to empty states. A further B doping will create additional D^+ states as a pair of B_4^- or as a result of a thermodynamical requirement.[26] These D^+ states can be observed to increase by the SCLPC measurement because they are assumed to be located above E_{f0} and can trap electrons.

As discussed above, the existing models proved to be insufficient to explain the modifications in $g(E)$ by light P and B doping, although these models are effective in the case that the Fermi level is significantly deviated from E_{f0}. More detailed study in the lower-ppm doping range is required to construct a comprehensive model which can account for the changes in $g(E)$ by the low-level doping as well as high-level doping.

V. SUMMARY AND CONCLUSIONS

We have developed the SCLPC technique, a new method to determine the DOS in the band gap, and applied it to the determination of the DOS of lightly P- and B-doped *a*-Si:H. This technique uses samples with blocking contacts such as Schottky or hetero contacts, and therefore, suffers essentially no dopant contamination from the highly doped layers which have been used for the conventional SCLC technique.

First we explained the principle of the technique in detail. Furthermore, we postulated three conditions: (1) $I_d \ll I_{ph}$, (2) $\alpha L \gg 1$, (3) $\mu\tau F \ll L$, to be satisfied in order to deduce meaningful $g(E)$ values. Next, we presented data with regard to the certainty of $g(E)$ deduced from the technique. The scaling law which ensures bulk or space-charge-controlled current was checked and found to be satisfied. The importance of interposing a thin doped layer between the transparent contact and the bulk layer to trap the photogenerated carriers was stressed in cases where the $\mu\tau$ value is large.

The energy profiles of $g(E)$ for the undoped and lightly P- and B-doped *a*-Si:H films deduced from the SCLPC technique were found to be qualitatively in agreement with the other data for the DLTS, CPM, and PDS techniques, and were generally explained by the existing models. The increase in $g(E)$ above E_{f0} by light B doping (≥ 3 vppm) was also explained by the existing models. However, the decrease in $g(E)$ below E_{f0} by light B doping (<1 vppm) found in the present measurement was not explained, but was explained by the model which we previously proposed.

[1] W. den Boer, J. Phys. (Paris) **C4**, 451 (1981).

[2] K. D. Mackenzie, P. G. LeComber, and W. E. Spear, Philos. Mag. B **46**, 377 (1982).

[3] I. Solomon, R. Benferhat, and H. Tran-Quoc, Phys. Rev. B **30**, 3423 (1984).

[4] S. Gangopadhyay, B. Schröder, and J. Geiger, Philos. Mag. B **56**, 321 (1987).

[5] H. Kakinuma, M. Mouri, M. Sakamoto, and H. Sawai, J. Appl. Phys. **67**, 558 (1990).

[6] F. J. du Chatenier, Philips Res. Rep. **23**, 142 (1968).

[7] P. Mark and W. Helfrich, J. Appl. Phys. **33**, 205 (1962).

[8] S. Ishioka, *Semiconductors and Semimetals,* edited by J. I. Pankove (Academic, Orlando, 1984), Vol. 21, Pt. D, p. 83.

[9] S. C. Lee, J. Appl. Phys. **55**, 4426 (1984).

[10] H. Sakai, M. Kamiyama, Y. Uchida, and H. Haruki, J. Non-Cryst. Solids **59/60**, 1151 (1983).

[11] H. Kakinuma, M. Sakamoto, Y. Kasuya, and H. Sawai, IEEE Trans. Electron. Devices **37**, 128 (1990).

[12] R. S. Crandall, *Semiconductors and Semimetals,* edited by J. I. Pankove (Academic, Orlando, 1984), Vol. 21, Pt. B, p. 245.

[13] P. N. Murgatroyd, Thin Solid Films **17**, 335 (1973).

[14] H. Kakinuma, Y. Kasuya, M. Sakamoto, and S. Shibata, J. Appl. Phys. **65**, 2307 (1989).

[15] S. Nešpurek and J. Swarakowski, J. Appl. Phys. **51**, 2099 (1980).

[16] W. B. Jackson, C. C. Tsai, and S. M. Kelso, J. Non-Cryst.

Solids **77/78**, 281 (1985).
[17]J. M. Marshall, R. A. Street, M. J. Thompson, and W. B. Jackson, Philos. Mag. B **57**, 387 (1988).
[18]X. Xu, A. Morimoto, M. Kumeda, and T. Shimizu, Jpn. J. Appl. Phys. **26**, L1818 (1987).
[19]Z. E. Smith, V. Chu, K. Shepard, S. Aljishi, D. Slobodin, J. Kolodzey, S. Wagner, and T. L. Chu, Appl. Phys. Lett. **50**, 1521 (1987).
[20]D. V. Lang, J. D. Cohen, and J. P. Harbison, Phys. Rev. B **25**, 5285 (1982).
[21]K. Pierz, B. Hilgenburg, H. Mell, and G. Weiser, J. Non-Cryst. Solids **97/98**, 63 (1987).
[22]K. Winer, I. Hirabayashi, and L. Ley, Phys. Rev. B **38**, 7680 (1988).
[23]J. Kočka, M. Veněček, and F. Schauer, J. Non-Cryst. Solids **97/98**, 715 (1987).
[24]G. Nobile and T. J. McMahon, J. Appl. Phys. **67**, 478 (1990).
[25]J. Kočka, J. Non-Cryst. Solids **90**, 91 (1987).
[26]K. Winer, Phys. Rev. Lett. **63**, 1487 (1989).
[27]M. Stutzmann, D. K. Biegelsen, and R. A. Street, Phys. Rev. B **35**, 5666 (1987).